

Network graph theory perspective on skeletal structures for theoretical and educational purposes

Ta'aseh Nevo and Dr. Shai Offer
Department of Mechanics Materials and Systems
Faculty of Engineering
Tel Aviv University

Keywords: skeletal structures, conjugate theorem, Tellegen's theorem, graph theory, system education

Notations

Abbreviations:

GR graph representation.
RGR resistance graph representation.
p.d. potential difference.

Symbols:

A member cross-section area.
 \mathbf{B} circuit matrix.
CF controlled-flow edge.
CP controlled-potential difference edge.
 \mathbf{d} member local deformation vector.
 E edge group.
 E member modulus of elasticity.
 \mathbf{f} member local force vector.
 F, \mathbf{F} flow/flow vector when related to a graph edge.
 F, \mathbf{F} force/force vector when related to a structural joint.
 $F_{t \rightarrow h}$ flow in edge with tail vertex t and head vertex h .
 \mathbf{G} graph.
 \mathbf{H} hybrid relation matrix.
 I member cross section moment of inertia.
 \mathbf{I} unity matrix.
 \mathbf{K} member local stiffness matrix.
 \mathbf{K}^R conductance of a resistance edge.
 L member length component.
 \mathbf{L} member length vector.
 P external force component or flow source edge.
 \mathbf{P} external force vector.
 P flow source edge set.
 \mathbf{Q} cutset matrix.
 \mathbf{R} member local flexibility matrix.
 R resistance edge.
 R^R resistance of a resistance edge.
 \mathbf{T} orthogonal transformation operator.
 Δ component of potential-difference or potential difference source edge.
 Δ potential-difference vector.
 $\boldsymbol{\pi}$ potential vector.
 $\boldsymbol{\Pi}$ matrix-vector of potentials

Superscripts:

A	angular.
CF	controlled-flow edge.
CP	controlled-potential difference edge.
F	flow aspect.
F	flow edge group.
L	linear.
P	flow source edge.
R	resistance edge.
t	matrix transpose operator.
Δ	potential aspect or potential source edge.

Subscripts:

h	head joint or vertex.
t	tail joint or vertex.
x,y,z	primal space directions.
ϕ,θ,ψ	Eulerian angles.

Matrix and Vector notations:

- Matrices and vectors of variables are designated with bold letters.
- Variables constituting vectors in space are designated with upper arrows.
- Vectors or matrices comprising variables constituting vectors in space are designated with bold letters and upper arrows.

Abstract

The paper introduces an approach, according to which skeletal structures are represented by a discrete mathematical model called graph representation. The paper shows that the reasoning upon the structure can be performed solely upon the representation, which besides the theoretical value, presents a powerful educational tool.

The paper shows that the students can learn skeletal structures entirely through the graph representations and to derive advanced structural topics, including the conjugate theorem and the unit force method from the theorems and principles of network graph theory.

The graph representations used in the paper for structures have been also applied to represent other engineering systems from different engineering disciplines. This enables to provide the students with a multidisciplinary perspective on analysis of engineering systems in general and skeletal structures in particular.

1. Introduction

The work reported in the paper is a part of a research approach, in which general discrete mathematical representations, called graph representations (GR), are being developed and then associated with a wide scope of engineering systems. Doing so leads to ability to substitute the reasoning over the engineering system by a more mathematically established reasoning over the graph representation. Accordingly, the results reported in the paper are not limited only to structural mechanics, but can be applied to other engineering disciplines that can be represented by the same representations. A GR isomorphic to an engineering system is capable of replacing the system in the analysis procedures and other forms of engineering reasoning. Due to the mathematical nature of the GR, using them instead of the original system would facilitate the computerizing and the systemizing of all the processes needed to be performed upon the system (Shai, 2001b). The generality of the work enables treating a variety of disciplines using a unified system of representations.

Current paper refers by term ‘graph representation’ to the graphs, which in addition to the basic graph-theory theorems and properties, possess special mathematical knowledge. Different knowledge content yields different types of graph representations. During years of research, a number of types of graph representations have been distinguished (Shai, 2003) and their correspondence to various engineering domains has been proved. Furthermore, it was found that some types of graph representations are interrelated through strong mathematical connections (Shai 2001a, Shai 2002), as depicted in the three-dimensional diagram shown in Fig. 1. The diagram comprises graph representations (designated by cubes to emphasize the existence of the embedded knowledge), engineering domains and all the possible interrelations. Since the graph representations constitute a more abstract mathematical level, in the diagram they appear above the level of graph representations. Also, some representations were shown to be more general than the others, thus in the diagram they appear at different heights.

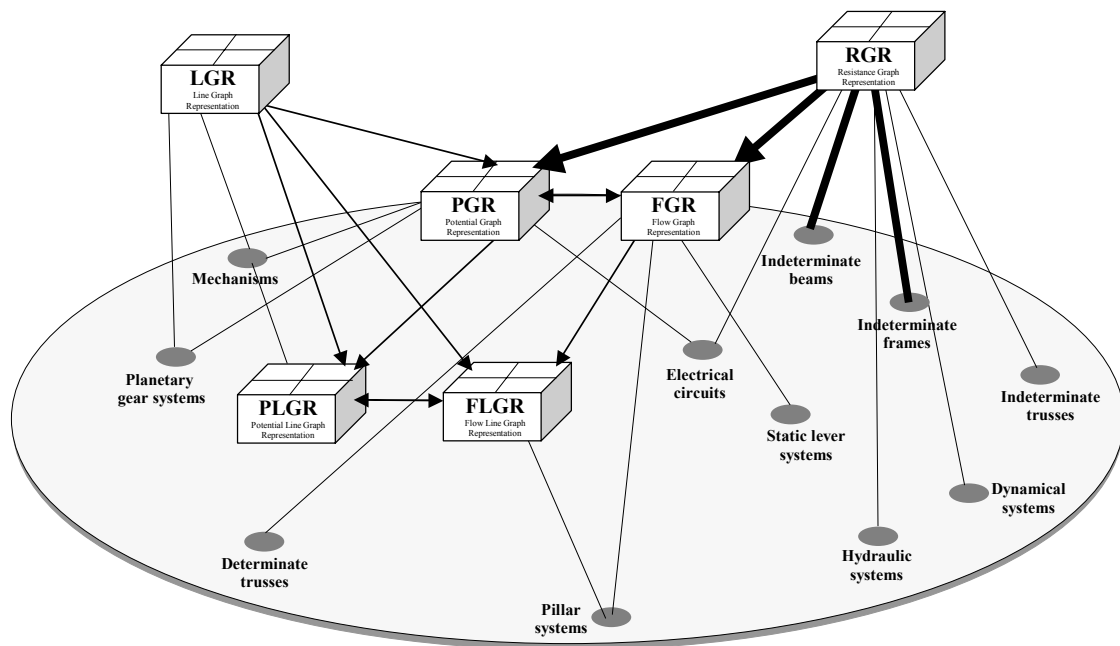


Figure 1. Hierarchic map of graph representations and engineering systems

Once an engineering system is represented by a graph representation, all the reasoning upon the system can be substituted by the reasoning over the graph representation. Since different engineering systems are treated in the same systematic way, the approach can significantly facilitate multidisciplinary research. So far, the approach has yielded a number of practical and theoretical applications that were described in previous publications, as follows: analysis of integrated engineering systems (Shai and Rubin, 2003), systematic design of engineering systems (Shai, 2003), finding relations between different engineering fields (Shai, 2001a; Shai, 2002), establishing new ways of collaboration between engineers from different fields (Shai 2003), deriving known and new theorems and methods in different engineering domains (Shai, 2003), establishing relations between different known methods in engineering (Shai, 2001b) and checking validity of engineering systems (Shai and Preiss, 1999).

Thick lines in Fig. 1 highlight the new relations that are employed in the current paper. Adding the beams and the frames to the group of engineering domains, to which graph representations are applicable, opens an avenue for new applications.

It can be seen from the figure that the graph representation chosen for beams and the frames is the Resistance Graph Representation (RGR). Actually, the same method that was applied for representing and analyzing integrated systems (Shai and Rubin, 2003) has been applied here to

frames and beams giving rise to the possibility of perceiving structural view within integrated systems consisting of control elements. Due to the research described here, beam and frame elements can also be embedded in such systems. This issue is especially important for systems belonging to MEMS, where the usage of beam and frame elements is quite frequent, due to limitations of the production process. Example of such a system and its graph representation is shown in Fig 2.

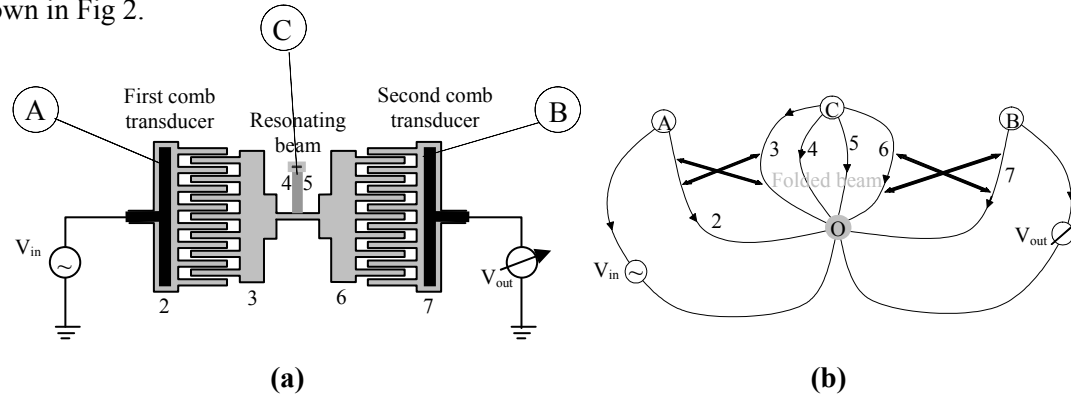


Figure 2. Microresonator and its graph representation.

The common treatment of skeletal structures in the last 50 years was based mainly on algebraic topology, first formulated by Langefors (1961), on the basis of structural matrix formulation (Southwell, 1940) and Roth's Diagram (Roth, 1955). This simple formulation of the structural knowledge was adopted and evolved by Spillers (1963), Wang and Bjørke (1991) and Kaveh, (1995) where the latter was the first to use matroid theory in structures. Nevertheless, this algebraic topology, although efficient for analysis of common structures, cannot be regarded as a network model, since it employs the structural framework incidence matrix, and such "Incidence Matrices have nothing whatever to do with Kirchhoff's Laws" (Kron, 1963). That is why Kron used his experience and knowledge in electricity to represent structures by electric circuits. Although satisfying Kirchhoff's Laws, these cumbersome 'mechanical' circuits were too complicated for analysis purpose. Fenves and Branin (1963) tried to apply network characteristics to Langefors' Algebraic Topology, and distinguished the part of this topology that obeys the two fundamental network laws from the part that does not, but kept on using this topology as is, and even implemented this method in a computer program called STRESS (Fenves et al., 1964), later evolved to STRUDL.

As graph representations enable one to achieve a new insight into different disciplines, this idea was applied to the development of a new teaching method by which students are first taught the graph representations, and only then do they learn the engineering material. Due to this new way of teaching, students have learned the engineering material from a new multidisciplinary perspective. Until now, more than 250 students have already participated in this course (Shai, 2001b). The work reported in this paper is one of the outcomes of this project.

2. Representing structural skeletal member by a graph

Current section is dedicated to the development of an isomorphic representation of a linear, conservative, elastic skeletal member, under the assumption of small angular displacements (McGuire and Gallagher, 1979). The representation, which will be referred as the Resistance Graph Representation – RGR (Shai, 2003), constitutes a directed graph (Swamy and Thurairaman, 1982) augmented by additional mathematical properties that will be explained in detail in the course of the paper. The paper distinguishes between two aspects of the representation – the so-called 'flow' representation and the 'potential' representation (Shai, 2001a; Shai, 2003). The flow graph representation is focused on the equations underlying the behavior of forces and the moments in the structure and the potential representation is focused on the equations underlying the behavior of deformations in the structure.

2.1. Representing the static behavior of a skeletal member through flows.

Each edge in the graph representation is associated to a vector variable called ‘flow’ (Shai, 2003). The flows of the graph satisfy the ‘flow law’, stating that the sum of flows in each vertex (or cutset) is equal to zero. In the paper, the flows are seen as comprised from two components: ‘linear flow’ oriented in the plane of the represented structure and ‘angular flow’ oriented perpendicularly to that plane.

Consider a spatial skeletal member shown in Fig. 3a. Its length and direction define a vector \mathbf{L} , and its end joints are denoted by t (tail) and h (head). The members considered here are acted upon by forces and moments exclusively at their end joints, therefore, when representing a structure by a graph we shall correspond a member and its end joints by two vertices, t and h , that are connected by a directed edge, called ‘the member edge’, as shown in Fig. 3b.

The member is subjected to two types of loads – a linearly-directed force, ${}^L\mathbf{F}$, and a moment, ${}^A\mathbf{F}$, also termed as angular force. The linear forces applied to the tail and head joints are in static equilibrium, thus:

$${}^L\mathbf{F}_t = -{}^L\mathbf{F}_h \quad (1)$$

In accordance with (1), it can be defined that the linear force acting on the tail joint, ${}^L\mathbf{F}_t$, corresponds to a linear flow associated with the corresponding member edge, as is depicted in Fig 3b. By (1), this flow corresponds also to the force applied by the head joint of the member to the beam elements it is interfaced with. The linear flow through the member edge is therefore defined as follows:

$${}^L\mathbf{F}_{t \rightarrow h} = {}^L\mathbf{F}_t = -{}^L\mathbf{F}_h \quad (2)$$

The moment or angular force, ${}^A\mathbf{F}$, cannot be represented in the same way, since the angular force applied to the tail joint is not equal to that applied to the head joint, as can be seen from the equilibrium of moments:

$${}^A\mathbf{F}_t = -{}^A\mathbf{F}_h - \mathbf{L} \times {}^L\mathbf{F}_h \quad (3)$$

The first component in the right hand side of Eq. (3) can be treated in the same way as the linear forces, by defining an angular component of a flow through the member edge that corresponds to the moment applied by the member to its head joint:

$${}^A\mathbf{F}_{t \rightarrow h} = -{}^A\mathbf{F}_h \quad (4)$$

The additional cross-product of the length vector, \mathbf{L} , by the linear force, ${}^L\mathbf{F}_h$, of Eq. (3) equilibrates a part of the angular tail force, without affecting the head joint. Therefore, this issue can be represented in the graph by a flow from the tail vertex through another edge, called ‘auxiliary edge’, into a common reference vertex, denoted by \mathbf{o} , that represents the ground, as shown in Fig. 3c. The flow law for the vertex t will then satisfy the condition stated in (3).

The angular flow in the auxiliary edge is dependent on the linear component of the flow through the member edge, thus constitutes a Flow-Controlled Flow Source. The variables corresponding to this edge will be denoted by the superscript CF (Controlled Flow), as shown in Fig. 3c. The angular flow through the auxiliary edge is given by:

$${}^A\mathbf{F}^{CF} = -\mathbf{L} \times {}^L\mathbf{F}_h = \mathbf{L} \times {}^L\mathbf{F}_{t \rightarrow h} \quad (5)$$

or, for three dimensional case in Cartesian coordinates:

$${}^A\mathbf{F}^{\text{CF}} = \mathbf{L} \times {}^L\mathbf{F}_{t \rightarrow h} = \begin{bmatrix} \hat{\mathbf{x}} & \hat{\mathbf{y}} & \hat{\mathbf{z}} \\ L_x & L_y & L_z \\ {}^L\mathbf{F}_{t \rightarrow h_x} & {}^L\mathbf{F}_{t \rightarrow h_y} & {}^L\mathbf{F}_{t \rightarrow h_z} \end{bmatrix} = \begin{bmatrix} \circ & -L_z & L_y \\ L_z & \circ & -L_x \\ -L_y & L_x & \circ \end{bmatrix} \cdot \begin{bmatrix} {}^L\mathbf{F}_x \\ {}^L\mathbf{F}_y \\ {}^L\mathbf{F}_z \end{bmatrix}_{t \rightarrow h} = {}^L\mathbf{A}\mathbf{H}^{\text{F}} \cdot {}^L\mathbf{F}_{t \rightarrow h} \quad (6)$$

whereas the linear flow through that edge is defined to be zero. The matrix ${}^L\mathbf{A}\mathbf{H}^{\text{F}}$ of Eq. (6) is the matrix characterizing the hybrid relation between the flows in the two edges. It should be noted that the transformation is performed between the linear flow in one edge to the angular flow in the other.

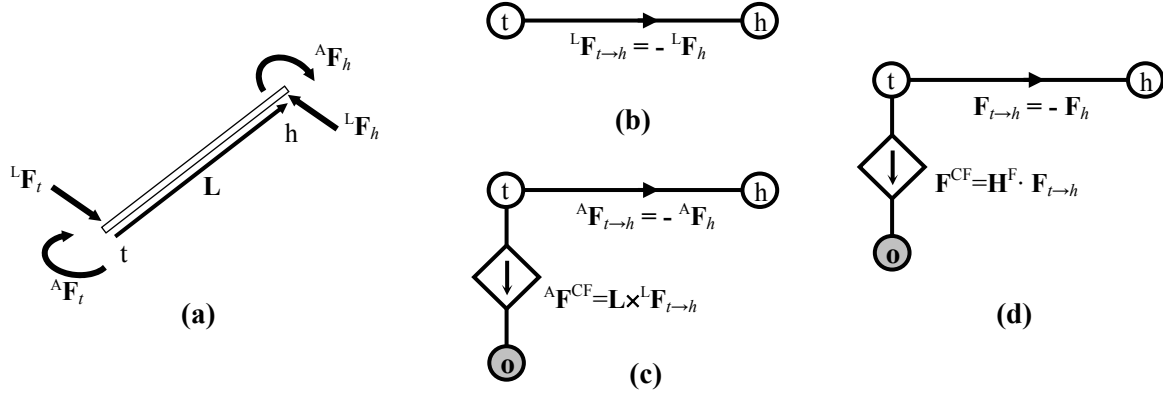


Figure 3. Forces in a structural skeletal member and their flow representation in a graph

(a) The skeletal member. (b) The linear flows in the member. (c) The angular flows of the member. (d) A complete flow representation of the member forces.

Figure 3d presents the resultant representation of the static aspects of a structural member. This representation comprises two edges - the member edge and the auxiliary dependent flow source.

For algebraic convenience, the two components of flow in the graph edges, although being of different types and units, can be written as a single multicommodity flow vector:

$$\mathbf{F}_j = \begin{bmatrix} {}^L\mathbf{F} \\ {}^A\mathbf{F} \end{bmatrix}_j = \begin{bmatrix} {}^L\mathbf{F}_x \\ {}^L\mathbf{F}_y \\ {}^L\mathbf{F}_z \\ {}^A\mathbf{F}_x \\ {}^A\mathbf{F}_y \\ {}^A\mathbf{F}_z \end{bmatrix}_j \quad (7)$$

Accordingly, (2) and (4) can be combined to give the total interpretation of the flow in the member edge:

$$\mathbf{F}_{t \rightarrow h} = -\mathbf{F}_h \quad (8)$$

while (6) can be rewritten for the auxiliary edge:

$$\mathbf{F}^{\text{CF}} = \mathbf{H}^{\text{F}} \cdot \mathbf{F}_{t \rightarrow h} \quad (9)$$

with the hybrid matrix \mathbf{H}^{F} given by:

$$\mathbf{H}^F = \begin{bmatrix} \circ & \circ & \circ & | & \circ & \circ & \circ \\ \circ & \circ & \circ & | & \circ & \circ & \circ \\ \circ & \circ & \circ & | & \circ & \circ & \circ \\ \hline \circ & -L_z & L_y & | & \circ & \circ & \circ \\ L_z & \circ & -L_x & | & \circ & \circ & \circ \\ -L_y & L_x & \circ & | & \circ & \circ & \circ \end{bmatrix} \quad (10)$$

2.2. Representing kinematic behavior of the skeletal member through potentials.

Each vertex in the representation is associated a vector variable, $\boldsymbol{\pi}$, called ‘potential’. Furthermore, each graph edge is assigned a vector called potential difference that is defined as a difference between the tail potential and the head potential of the edge:

$$\Delta_{t \rightarrow h} = \boldsymbol{\pi}_t - \boldsymbol{\pi}_h \quad (11)$$

Each joint in the structure may be displaced from its original position due to a change of the state of self-stress, and/or externally applied loads. Like the forces, the displacements in a structure include both linear and angular components, constituting a linear displacement of the member and its acquired slope at some point. In the graph, this displacement is represented by a potential, $\boldsymbol{\pi}$, associated with the corresponding graph vertex. Thus, the potentials and the potential differences of the graph are also composed of linear and angular components.

The linear and angular potential differences across the member edge, given by (11), represent the linear and angular relative displacements between the end joints of the corresponding member. The linear relative displacement is contributed by two effects, depicted in Fig. 4a. The first effect is a rigid body rotation of the member, whose contribution to the linear relative displacement depends on the degree of the angular displacement represented by the angular potential of the tail vertex. This dependence effect can be implemented in the graph as a Potential Controlled Potential difference Source, whose variables are designated by superscript CP (Controlled Potential). The expression for this potential difference, ${}^L\Delta^{CP}$, will be developed later in this section.

The second linear effect is the elastic deformation of the member, whose contribution to the linear relative displacement is linearly dependent on both the linear and angular internal forces of the member. Such relation is represented by a linear relation between potential difference and flow, referred to, in this type of graph representation, as the resistance of the corresponding edge (Shai 2001b). Therefore, the linear relative displacement caused by deformation will be referred to in its graph representation as a resistance linear potential difference, and will be denoted by ${}^L\Delta^R$.

The linear potential difference across the member edge is therefore:

$${}^L\Delta_{t \rightarrow h} = {}^L\Delta^{CP} + {}^L\Delta^R \quad (12)$$

Unlike the linear relative displacement, the angular relative displacement, i.e. the difference between the angular displacements of the member end joints, is strictly the angular deformation (Fig. 4b), referred to in its graph representation as the resistance angular potential difference, ${}^A\Delta^R$. Since only small angles are considered, the commutative property is valid when represented as vectors (Goldstein, 1950), hence the vector of angular potential difference can be given by:

$${}^A\Delta_{t \rightarrow h} = {}^A\boldsymbol{\pi}_t - {}^A\boldsymbol{\pi}_h = {}^A\Delta^R \quad (13)$$

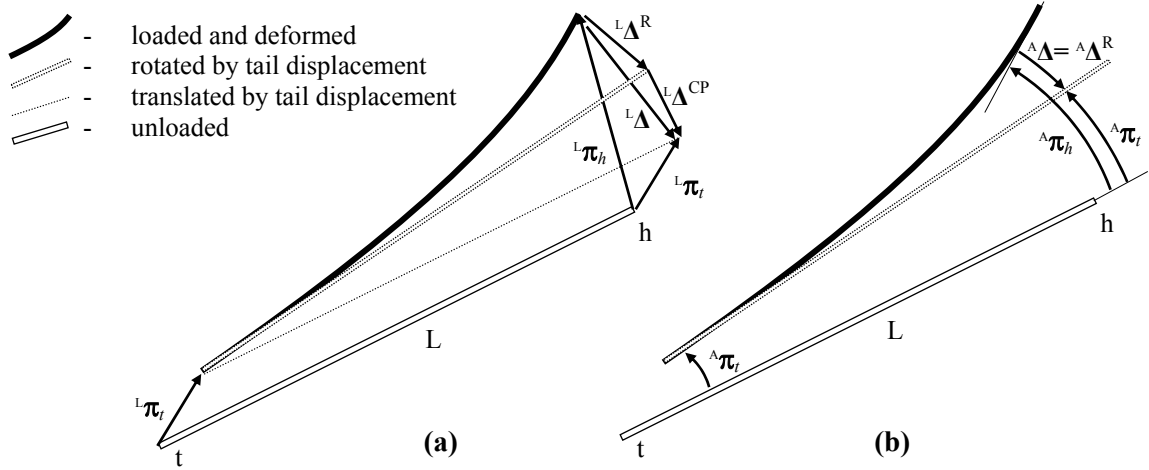


Figure 4. Linear and angular displacements in a structural member

(a) Linear displacements. (b) Angular displacements.

The expressions (12) and (13) can be generalized into a single potential difference vector presentation, as follows:

$$\begin{bmatrix} L \Delta \\ A \Delta \end{bmatrix}_{t \rightarrow h} = \begin{bmatrix} L \Delta \\ A \Delta (= \mathbf{0}) \end{bmatrix}^{CP} + \begin{bmatrix} L \Delta \\ A \Delta \end{bmatrix}^R, \quad \text{or: } \Delta_{t \rightarrow h} = \Delta^{CP} + \Delta^R \quad (14)$$

Since the potential difference of the member edge is composed of two different types, as is seen in (14), the member edge is to be replaced by a couple of serial edges: a dependent potential source – CP, and a resistance edge – R.

In order to represent the integrated static-kinematic behavior of a structural member, we shall combine the graph properties obtained till now into a unified representation. The resulted graph, shown in Fig. 5, represents both flows and potential differences, and can therefore be referred to as the resistance representation of the structural member (Shai, 2003). The term 'member edge' will now refer to both CP and R edges as a pair. Due to their serial connection, the flow through the member edge, $F_{t \rightarrow h}$, is equal in both of its components, CP and R edges, i.e.

$$\mathbf{F}^{CP} = \mathbf{F}^R = \mathbf{F}_{t \rightarrow h} \quad (15)$$

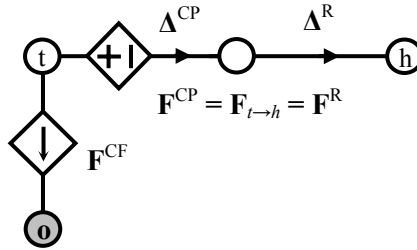


Figure 5. The Resistance element graph corresponding to a structural member

The explicit expressions for Δ^{CP} and Δ^R are now to be developed, starting with Δ^R , the resistance potential difference representing the elastic deformation effect.

The deformation of a member, Δ^R , is accumulated through the effect of the internal forces in each section along the member. However, it is well-known that since internal forces along the member can be determined by the force at the head vertex (\mathbf{F}^R) alone, the deformation can directly be related to this force.

The relation between force and deformation is independent on the coordinate system, but most conveniently it can be formulated through the local coordinate system of the member. Several ways to select this local system were introduced in the literature (Fleming, 1989), many of them (Spillers, 1963; Fuchs, 1992) decompose global vectors into essentially different local components, and even use both tail and head components simultaneously. In order to maintain the nature of vectors through the transformation, the way of McGuire and Gallagher (1975) is adopted in this paper, according to which the local system is merely a global-like system, whose axes are oriented along the primal directions of the member, as is formulated in (16):

$$\Delta^R = \mathbf{R}^R \cdot \mathbf{F}^R; \quad \mathbf{F}^R = \mathbf{K}^R \cdot \Delta^R \quad (16)$$

where \mathbf{R}^R and $\mathbf{K}^R = (\mathbf{R}^R)^{-1}$ are respectively the resistance and conductance matrices of the member edges, which can be obtained by similarity transformation of the local flexibility/stiffness matrices:

$$\mathbf{R}^R = \begin{bmatrix} \mathbf{T}' & \circ \\ \circ & \mathbf{T}' \end{bmatrix} \cdot \begin{bmatrix} {}^{LL}\mathbf{R} & {}^{AL}\mathbf{R} \\ {}^{LA}\mathbf{R} & {}^{AA}\mathbf{R} \end{bmatrix} \cdot \begin{bmatrix} \mathbf{T} & \circ \\ \circ & \mathbf{T} \end{bmatrix}; \quad \mathbf{K}^R = \begin{bmatrix} \mathbf{T}' & \circ \\ \circ & \mathbf{T}' \end{bmatrix} \cdot \begin{bmatrix} {}^{LL}\mathbf{K} & {}^{AL}\mathbf{K} \\ {}^{LA}\mathbf{K} & {}^{AA}\mathbf{K} \end{bmatrix} \cdot \begin{bmatrix} \mathbf{T} & \circ \\ \circ & \mathbf{T} \end{bmatrix} \quad (17)$$

Where \mathbf{T} is the orthogonal operator relating between the local and the global coordinate systems.

As for the dependent potential source, Δ^{CP} , the potential difference is given, as can be seen in Fig. 4a, by:

$$\Delta^{CP} = {}^L\Delta^{CP} = \mathbf{L} \times {}^A\boldsymbol{\pi}_t \quad (18)$$

The potential difference in the dependent flow source edge, CF, is equal to the potential in the tail vertex, thus it can replace ${}^A\boldsymbol{\pi}_t$:

$${}^A\boldsymbol{\pi}_t = {}^A\Delta^{CF} \quad (19)$$

therefore (18) becomes:

$${}^L\Delta^{CP} = \mathbf{L} \times {}^A\Delta^{CF} \quad (20)$$

Eq. (20) can be rewritten as a matrix multiplication:

$${}^L\Delta^{CP} = {}^{AL}\mathbf{H}^\Delta \cdot {}^A\Delta^{CF} \quad (21)$$

where, similarly to (6):

$${}^{AL}\mathbf{H}^\Delta = {}^{LA}\mathbf{H}^F = \begin{bmatrix} \circ & -L_z & L_y \\ L_z & \circ & -L_x \\ -L_y & L_x & \circ \end{bmatrix} \quad (22)$$

and so (21) can be generalized to give:

$$\Delta^{CP} = \mathbf{H}^\Delta \cdot \Delta^{CF} \quad (23)$$

Where the potential difference vectors and the hybrid potential difference relation matrix, \mathbf{H}^Δ , are given by:

$$\Delta_j = \begin{bmatrix} L \Delta \\ A \Delta \end{bmatrix}_j = \begin{bmatrix} L \Delta_x \\ L \Delta_y \\ L \Delta_z \\ A \Delta_x \\ A \Delta_y \\ A \Delta_z \end{bmatrix}_j ; \quad \mathbf{H}^\Delta = \begin{bmatrix} \circ & \circ & \circ & \circ & -L_z & L_y \\ \circ & \circ & \circ & L_z & \circ & -L_x \\ \circ & \circ & \circ & -L_y & L_x & \circ \\ \hline \circ & \circ & \circ & \circ & \circ & \circ \\ \circ & \circ & \circ & \circ & \circ & \circ \\ \circ & \circ & \circ & \circ & \circ & \circ \end{bmatrix} \quad (24)$$

One can notice that the hybrid matrices \mathbf{H}^Δ and \mathbf{H}^F are related to each other as follows:

$$\mathbf{H}^\Delta = -(\mathbf{H}^F)^t \quad (25)$$

After partitioning the member edge, (9) can be restated as follows:

$$\mathbf{F}^{CF} = \mathbf{H}^F \cdot \mathbf{F}^{CP} \quad (26)$$

According to (26) and (23), the flow in CF is controlled by the flow in CP, while the potential difference in CP is controlled by the potential difference in CF. Consequently, the member can now be represented by a more inclusive resistance element graph, shown in Fig. 6, where i stands for the index of the represented member of the structure. The graph is accompanied by its interrelations (16), (23) and (26).

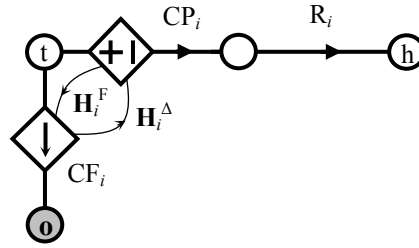


Figure 6. The resistance element graph corresponding to a skeletal member and its inner interrelations

Once the graph representation is established, all the topological rules which have been developed for this type of graph become available (Shai, 2003). One of such rules is the generality rule of the edge direction, stating that any edge direction can be reversed without loss of consistency, if the sign of the associated flow and potential difference vectors is reversed, too. It should be noted, though, that even when edge direction is reverted, the vector \mathbf{L} associated with each member edge remains unchanged for it is determined by the direction originating at the tail vertex, which is always the vertex connected with the auxiliary edge. Therefore, the matrices \mathbf{K}^R and \mathbf{R}^R are invariant in relation to edge directions. As for \mathbf{H}^Δ and \mathbf{H}^F , sign inversion should be applied to both whenever the direction is reversed in either CF or CP edges in order for the relations (23) and (26) to remain valid.

The graph appearing in Fig. 6 reflects both static and kinematical properties of the beam element. In the proposed educational technique it is suggested that the students are first taught this graph with all its mathematical properties and embedded methods. Only then are they taught that the graph can be interpreted as an isomorphic representation of a skeletal structure. It should be noted that the same graph can be interpreted as additional types of engineering systems (Shai 2003), thus once the graph-theoretical mathematical basis has been taught, the students can be exposed to a wide variety of engineering disciplines and gaining a multidisciplinary perspective.

2.3. Graph representation of a general skeletal structure.

A framework structure can be represented using a resistance graph by dividing the structure into primitive members, representing each member by an element graph and interconnecting these element graphs into a single graph in a certain topological manner. For example, consider the beam of Fig. 7a. The structure possesses three joints: 'A' and 'C' as joints of support, and 'B' as a joint upon which the external force is applied. Accordingly, two members are identified in the beam, as is depicted in the figure. Directions are assigned to the members as shown, and the graph representation of each of the members is constructed according to section 2. Joint B is a joint common to both of the members, thus the two member graphs are interconnected so that vertex B is their common vertex. Obviously, the reference vertex is also common to both members' element graphs.

Supports are represented as sources of zero potential in those dimensions where the motion is not possible. In the unconstrained dimensions, such as the angular z-dimension of the support at C, the joint has no connection to ground, therefore the flow from the corresponding vertex to the reference vertex in these dimensions is zero, and it is referred to as a resistance edge with a zero conductance. The external force is represented as a flow source edge between the reference vertex and the vertex corresponding to the joint B, directed from the reference vertex to the vertex B.

The obtained graph is a resistance graph representation of the structure. Its variables should satisfy the flow law, potential law and the member equations. These represent all the physical laws ruling the behavior of the structure, thus analysis of the graph behavior can totally replace the analysis of the structure, namely, the graph is isomorphic to the structure.

The graph is basically constructed, as shown in Fig. 7b, but, for the sake of convenience, an additional step can be taken at which the two parallel CF edges are merged into one, CF_{1+2} . Although they control different potential sources, being parallel, they possess the same potential difference. The simplified graph is shown in Fig. 7c.

Once the graph is constructed, the flow variables of the edges become part of a general circulation in the graph, originating in the flow sources, flowing through the edges to the reference vertex and then back to the sources.

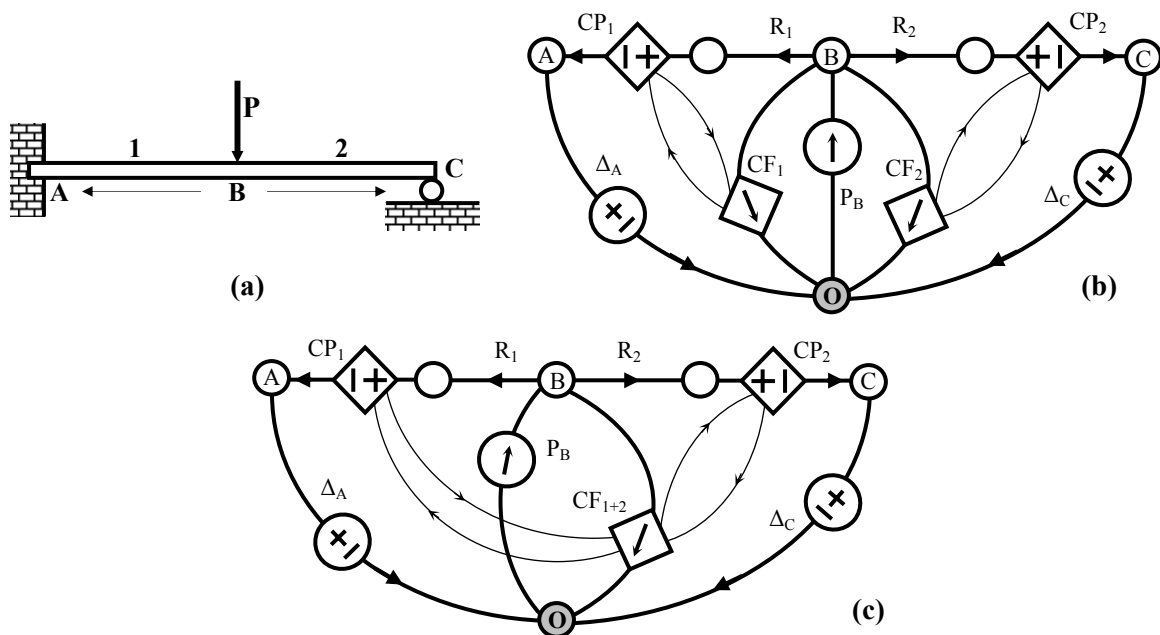


Figure 7. Graph Representation of a beam

(a) An indeterminate beam. (b) The corresponding graph representation. (c) Simplification of the graph by merging the parallel CF edges.

The process of constructing a graph representation of a skeletal structure is performed systematically, as is described in Algorithm 1:

Algorithm 1: Constructing a graph representation of a structure

1. Divide the structure to its primitive members.
2. Set a direction for each structural member.
3. Represent each structural member according to the graph appearing in Fig. 6, and each pin-jointed member (a rod) by a resistance edge. Connect all the edges through their end vertices according to the interconnections of the members in the structure, and combine all the reference vertices into one.
4. Represent each kinematical constraint by a potential difference source whose tail is the vertex corresponding to the constrained joint and its head is the reference vertex.
5. Represent each externally applied load by a flow source edge directed from the reference vertex to the vertex corresponding to the joint upon which the load is applied.
6. Merge parallel dependent flow sources, and contract potential sources forcing a zero potential in all dimensions (like clamped supports).

3. Applications

In previous sections, the isomorphic graph representation for a structure was developed. The representation was constructed in a way to ensure that the mathematical behavior of the representation completely reflects the physical behavior of the represented structure. Accordingly, possessing a representation of structure enables one to substitute any reasoning process over the structure by mathematical reasoning over the representation. The abilities arising as a consequence of this issue are discussed in this section.

3.1. Structural Analysis through Graph Representations.

One of the immediate applications of the graph representation of a skeletal structure is to structural analysis. Since the graph represents an engineering system isomorphically, the analysis can be performed directly upon the graph using known methods and algorithms that are embedded in the graph representation and mathematical interrelations with other representations.

One of these methods is the Mixed-Variable Method (Balabanian and Bickart, 1969), which is formulated in the terminology of the graph representations in (Shai and Rubin, 2003; Ta'aseh and Shai, 2002). Upon application to a graph representation, the Mixed-Variable Method divides the edges of the graph into two groups E^F and E^A to form two auxiliary graphs – G_F and G_A . From these graphs a straightforward procedure leads to a system of linear equations, whose unknowns are the flows in the chords of G_F and the potential differences in the branches of G_A . The variables underlying the original graph representations are then obtained from these variables through simple matrix multiplications. Figure 8 shows an example frame system. The structure is loaded as shown, and we consider a problem where the forces in the members should be determined, as well as the displacements of joints b and c. The problem shown here is widely used in the literature as an example demonstrating various methods for analysis of indeterminate skeletal structures (Southwell, 1940; Carter and Kron, 1944; tBjørke, 1995). Figure 9 shows the solution of this problem obtained by applying the Mixed Variable Method to the graph representation of this frame. More details on derivation of the analysis equations presented in Figure 9 can be found in (Ta'aseh and Shai, 2002).

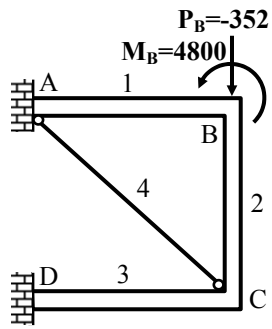
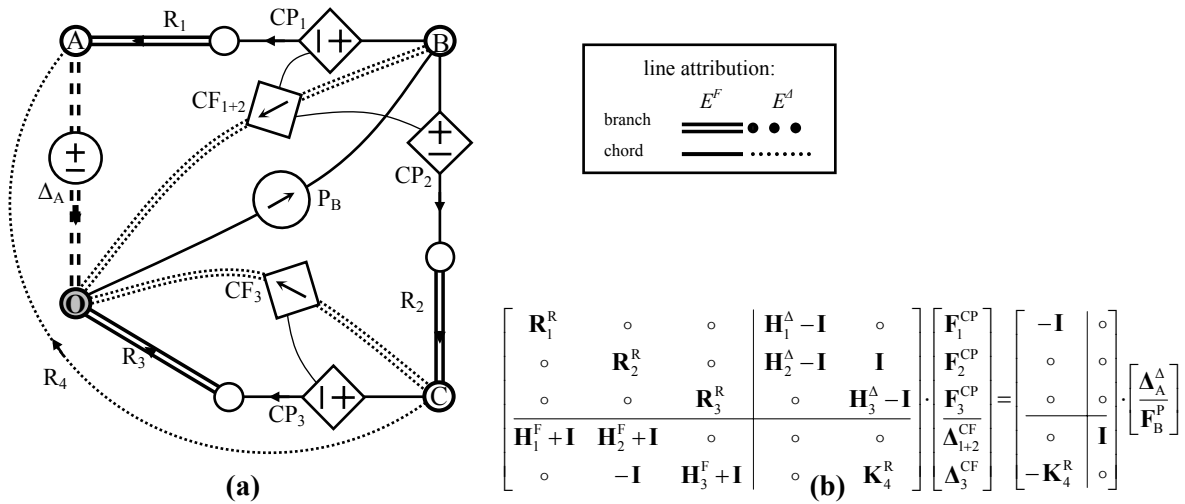


Figure 8. Example frame system to be analyzed.



$$\begin{bmatrix} \frac{L}{AE} & 0 & 0 & -1 & 0 & 0 \\ 0 & \frac{L^3}{3EI} & -\frac{L^2}{2EI} & 0 & -1 & L_1 \\ 0 & -\frac{L^2}{2EI} & \frac{L}{EI} & 0 & 0 & -1 \\ \frac{L^3}{3EI} & 0 & \frac{L^2}{2EI} & -1 & 0 & 0 \\ 0 & \frac{L}{AE} & 0 & 0 & -1 & L_2 \\ \frac{L^2}{2EI} & 0 & \frac{L}{EI} & 0 & 0 & 1 \\ \frac{L}{AE} & 0 & 0 & 0 & -1 & 0 \\ 0 & \frac{L^3}{3EI} & -\frac{L^2}{2EI} & 0 & 0 & -1 \\ 0 & -\frac{L^2}{2EI} & \frac{L}{EI} & 0 & 0 & -1 \\ -1 & 0 & 0 & -1 & 0 & 0 \\ 0 & -1 & 0 & 0 & -1 & 0 \\ 0 & L_1 & -1 & -L_2 & 0 & -1 \\ 1 & 0 & 0 & 0 & 1 & 0 \\ 0 & 0 & 1 & 0 & 0 & -1 \\ 0 & 0 & 0 & 0 & 0 & L_3 & -1 \end{bmatrix} \cdot \begin{bmatrix} F_1^{CP} \\ F_2^{CP} \\ F_3^{CP} \\ \Delta_{1+2}^{CF} \\ \Delta_3^{CF} \end{bmatrix} = \begin{bmatrix} -1 & 0 & 0 \\ 0 & -1 & 0 \\ 0 & 0 & -1 \\ 1 & 0 & 0 \\ 0 & 1 & 0 \\ 0 & 0 & 1 \\ 1 & 0 & 0 \\ 0 & -1 & 0 \\ 0 & 0 & -1 \\ 0 & 0 & 0 \\ 0 & 0 & 0 \\ 0 & 0 & 0 \\ 1 & 0 & 0 \\ 0 & 1 & 0 \\ 0 & 0 & 1 \end{bmatrix} \cdot \begin{bmatrix} \Delta_A \\ P_B \end{bmatrix}$$

elements 1,2,3:
 L = 50
 EA = 13,000
 EI = 16,250

truss rod 4:
 L = 70.7
 EA = 19,500

$$\mathbf{F}_B^P = \begin{bmatrix} 0 \\ -352 \\ 4800 \end{bmatrix}; \quad \begin{bmatrix} L F_{1x}^{CP} \\ L F_{1y}^{CP} \\ A F_{1z}^{CP} \\ L F_{2x}^{CP} \\ L F_{2y}^{CP} \\ A F_{2z}^{CP} \\ L F_{3x}^{CP} \\ L F_{3y}^{CP} \\ A F_{3z}^{CP} \end{bmatrix} = \begin{bmatrix} -54.75 \\ -80.71 \\ -1397 \\ 54.75 \\ -271.3 \\ -575.5 \\ -232.7 \\ 16.12 \\ 229.7 \end{bmatrix}; \quad \begin{bmatrix} L \Delta_{1+2x}^{CF} \\ L \Delta_{1+2y}^{CF} \\ A \Delta_{1+2z}^{CF} \\ L \Delta_{3x}^{CF} \\ L \Delta_{3y}^{CF} \\ A \Delta_{3z}^{CF} \end{bmatrix} = \begin{bmatrix} -0.2106 \\ -4.022 \\ 1.909 \\ -0.8948 \\ -2.979 \\ -0.5321 \end{bmatrix}$$

Figure 9. Solving a structural graph representation by Mixed Variable Method

- (a) The graph representation of the frame of Fig. 8.
- (b) The set of equations stemming from the Mixed Variable method in its vectorial form
- (c) The set of equations in the explicit form.
- (d) Given parameters.
- (e) The solution.

3.2. Applying Tellegen's theorem to structures.

In this section the well-known Tellegen's theorem will be applied to the RGR of a structure, and it will be shown that the result coincides with a known mechanical energy method. In (Shai, 2001c) the application of Tellegen's theorem to trusses was introduced, while here, through the graph representation developed in this paper, this theorem is extended to skeletal structures.

Tellegen's theorem was originally related to electrical networks (Tellegen, 1952). Later it was extended to a general orthogonality principle between two isomorphic vector-networks (Andrews, 1971). According to this extension, Tellegen's theorem can be stated using graph terminology as follows (Shai, 2001c):

Tellegen's Theorem: Let \mathbf{G}^Δ and \mathbf{G}^F be isomorphic potential and flow graphs. Then:

$$\sum_{j=1}^{e(\mathbf{G})} (\Delta_j^\Delta)^t \cdot \mathbf{F}_j^F = 0 \quad (27)$$

where $e(\mathbf{G})$ is the number of edges in the graph, Δ_j^Δ is the vectorial potential difference of the j -th edge in \mathbf{G}^Δ , and \mathbf{F}_j^F is the vectorial flow of the corresponding edge in \mathbf{G}^F .

As was shown in (Shai, 2001c), for truss graph representations, the expression in (27), when related to general structure graph representations can be decomposed as follows:

$$\sum_{j=1}^{e(\mathbf{G})} (\Delta_j^\Delta)^t \cdot \mathbf{F}_j^F = \sum_A (\Delta_A^\Delta)^t \cdot \mathbf{F}_A^F + \sum_P (\Delta_P^\Delta)^t \cdot \mathbf{F}_P^F + \sum_i (\Delta_i^\Delta)^t \cdot \mathbf{F}_i^F = 0 \quad (28)$$

where subscript A indicates upon potential difference source edges corresponding to constraints, subscript P upon the flow source edges corresponding to externally applied loads, and i indicates edges corresponding to the structural members. Superscripts Δ and F , as before, indicate relation to \mathbf{G}^Δ or \mathbf{G}^F , respectively. In constrained degrees of freedom the displacement is zero, therefore:

$$\Delta_A^\Delta = 0 \quad (29)$$

The degrees of freedom in which the support is free, are not constrained for potentials, but are free of forces, thus possess zero flow. Therefore, the first term in (28) becomes:

$$\sum_A (\Delta_A^\Delta)^t \cdot \mathbf{F}_A^F = 0 \quad (30)$$

As for the flow sources representing loads, each such flow source edge is directed from the reference vertex to the vertex corresponding to the loaded joint. So its tail potential is always zero, while the head potential corresponds to the displacement of the loaded joint. Therefore, by (11):

$$\Delta_P^\Delta = -\mathbf{\Pi}_P^\Delta \quad (31)$$

substituting (29) and (30) in (28) results in:

$$\sum_i (\Delta_i^\Delta)^t \cdot \mathbf{F}_i^F = \sum_P (\mathbf{\Pi}_P^\Delta)^t \cdot \mathbf{F}_P^F \quad (32)$$

At this stage, the Tellegen's theorem can be further adjusted for the structural graph representation developed in this paper. The left side of (32) is a summation over the structural member edges, while each member is represented by three edges: a resistance edge, a dependent potential source and a dependent flow source, as shown in Fig. 4. Hence, each term in the summation can be expanded into three, as follows:

$$(\Delta_i^\Delta)^t \cdot \mathbf{F}_i^F = (\Delta_R^\Delta)^t \cdot \mathbf{F}_R^F + (\Delta_{CP}^\Delta)^t \cdot \mathbf{F}_{CP}^F + (\Delta_{CF}^\Delta)^t \cdot \mathbf{F}_{CF}^F \quad (33)$$

Due to isomorphism between the potential and flow graphs upon which Tellegen's theorem is applied, it is suggested that the structural systems to which the graphs correspond are having the same topology. Moreover, for simplicity, the geometry of these systems is chosen to be identical.

Therefore, the hybrid matrices \mathbf{H}^Δ and \mathbf{H}^F of each member in the system represented by the potential graph are equal to those of the corresponding member in the system represented by the flow graph, and are interrelated to each other by (25). Applying hybrid connections (23) and (26) to (33) gives:

$$\left(\Delta_i^\Delta\right)^t \cdot \mathbf{F}_i^F = \left(\Delta_R^\Delta\right)^t \cdot \mathbf{F}_R^F + \left(\mathbf{H}^\Delta \cdot \Delta_{CF}^\Delta\right)^t \cdot \mathbf{F}_{CP}^F + \left(\Delta_{CF}^\Delta\right)^t \cdot \mathbf{H}^F \cdot \mathbf{F}_{CP}^F \quad (34)$$

And since $\mathbf{H}^F = (-\mathbf{H}^\Delta)^t$,

$$\left(\Delta_i^\Delta\right)^t \cdot \mathbf{F}_i^F = \left(\Delta_R^\Delta\right)^t \cdot \mathbf{F}_R^F + \left(\Delta_{CF}^\Delta\right)^t \cdot \left(\mathbf{H}^\Delta\right)^t \cdot \mathbf{F}_{CP}^F + \left(\Delta_{CF}^\Delta\right)^t \cdot \left(-\mathbf{H}^\Delta\right)^t \cdot \mathbf{F}_{CP}^F \quad (35)$$

The two right-most terms cancel each other, so:

$$\left(\Delta_i^\Delta\right)^t \cdot \mathbf{F}_i^F = \left(\Delta_R^\Delta\right)^t \cdot \mathbf{F}_R^F \quad (36)$$

The latter result indicates that each member contributes to equation (32) only a product term dependent on its resistance edge. Using the resistance relation (16), (35) can be rewritten as:

$$\left(\Delta_i^\Delta\right)^t \cdot \mathbf{F}_i^F = \left(\Delta_R^\Delta\right)^t \cdot \mathbf{F}_R^F = \left(\mathbf{R}_R^R \cdot \mathbf{F}_R^\Delta\right)^t \cdot \mathbf{F}_R^F = \left(\mathbf{F}_R^\Delta\right)^t \cdot \left(\mathbf{R}_R^R\right) \cdot \mathbf{F}_R^F = \left(\mathbf{F}_R^\Delta\right)^t \cdot \mathbf{R}_R^R \cdot \mathbf{F}_R^F \quad (37)$$

Where the last transition employs the resistance matrix symmetry. Substituting (36) into (32) gives:

$$\sum_R \left(\mathbf{F}_R^\Delta\right)^t \cdot \mathbf{R}_R^R \cdot \mathbf{F}_R^F = \sum_P \left(\Pi_P^\Delta\right)^t \cdot \mathbf{F}_P^F \quad (38)$$

The last expression relates flows in both graphs to the potentials of the vertices upon which the external loads are applied. As in Shai (2001c), this expression can be used to deduce theorems and techniques that were developed in structural mechanics on the basis of energy considerations, such as unit-force method and Betti's law.

For example, if a specific displacement in the structure is to be determined, the expression (38) can be further simplified by choosing the proper isomorphic potential and flow graphs, upon which Tellegen's theorem is applied. The potential graph, \mathbf{G}^Δ , is the derivative of the resistance graph that represents the structure in question, with an extra-edge connecting the reference vertex with the vertex whose displacement is to be determined (the flow in this extra-edge is set to zero to maintain the original flow balance). The flow graph, \mathbf{G}^F , is an isomorphic graph, in which all flow sources are set to zero, and a unit flow, \mathbf{P}^1 , is set in the extra-edge. This way, the sum of products over the flow sources in the form (38) of Tellegen's theorem includes only the product associated with the extra-edge, whose flow equals to $\mathbf{1}$ in the relevant dimension. Therefore, (38) becomes:

$$\Pi_{P^1}^\Delta = \sum_R \left(\mathbf{F}_R^\Delta\right)^t \cdot \mathbf{R}_R^R \cdot \mathbf{F}_R^F \quad (39)$$

One can notice that (39) coincides with the equation of the well-known unit-force method (Hibbeler, 1985). The application of the last equation is demonstrated here through an example problem, taken from (Hibbeler, 1985) p.247. In this problem, shown in Fig. 10a, the slope at point C of the beam is to be determined. The graphs \mathbf{G}^Δ and \mathbf{G}^F , constructed according to the description above, are shown in fig. 10b and 10c, respectively.

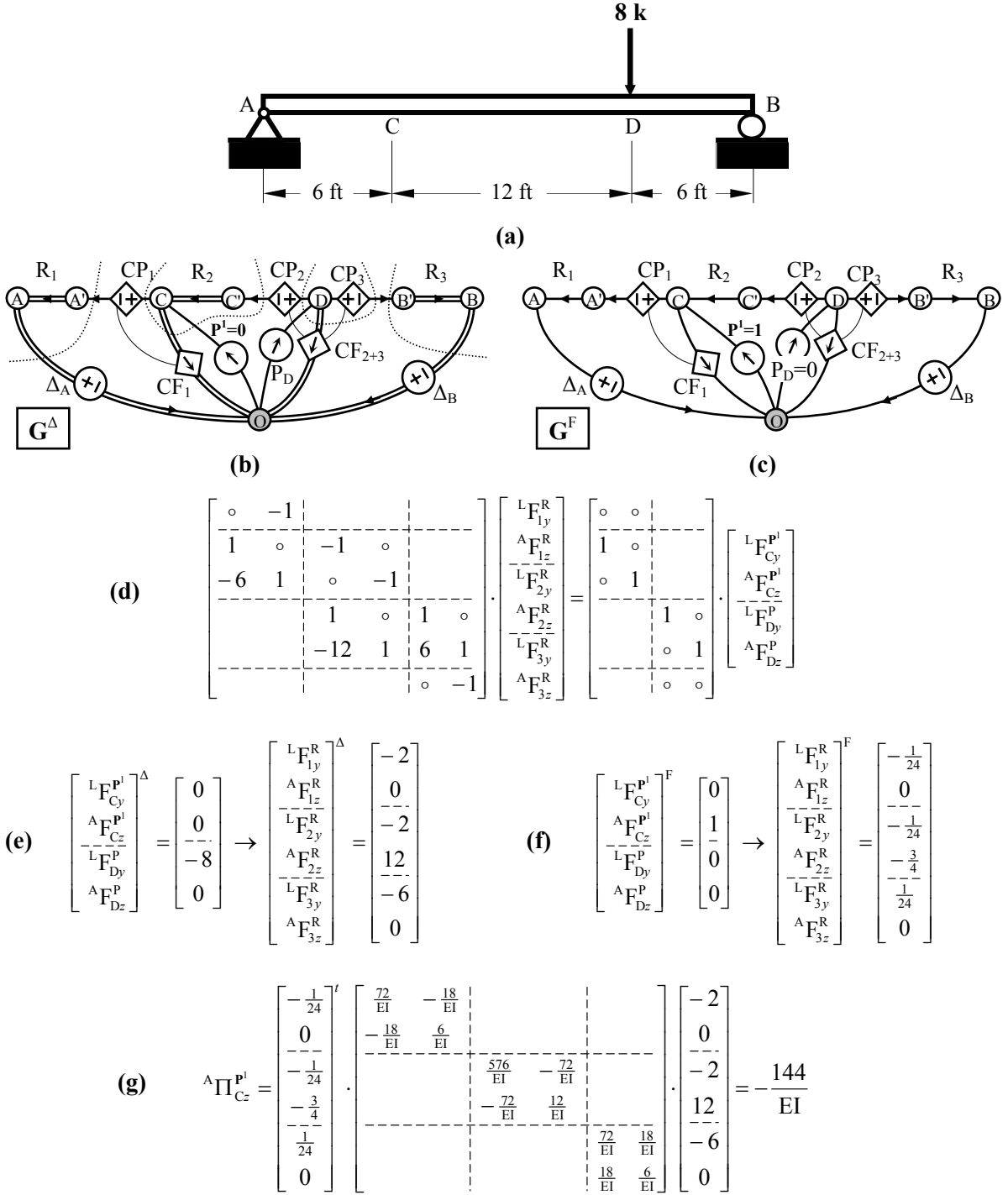


Figure 10. Application of Tellegen's theorem to a beam

(a) A simply supported beam. (b) The original graph as a potential graph. (c) An isomorphic graph as a flow graph, with a unit flow source directed to the vertex whose potential is to be determined. (d) The explicit flow law by Eq. (27). (e) The original graph flow solution. (f) The isomorphic graph flow solution. (g) The potential of the vertex in question determined using Tellegen's theorem.

The spanning tree used to formulate the flow law is identical in both graphs due to isomorphism and is shown for G^Δ in Fig. 10b. The flow law for the cutsets that disconnect the midway vertices A', B' and C', can be stated in general as follows:

$$\bar{\mathbf{F}}_R = \bar{\mathbf{F}}_{CP} \tag{40}$$

Relating to all other T' cutsets shown in fig. 10b, and using (40) and the hybrid connection (26), the flow law can be formulated through the following cutset equation:

$$\left(\bar{\mathbf{Q}}_{T'R} + \bar{\mathbf{H}}^F\right) \cdot \bar{\mathbf{F}}_R = -\bar{\mathbf{Q}}_{T'P} \cdot \bar{\mathbf{F}}_P \quad (41)$$

Applying (41) to the graphs in fig. 10b and 10c, with the hybrid relation matrices \mathbf{H}_i^F according to (10), results in the explicit equation of fig. 10d. Substituting the appropriate source flows for the graphs of fig. 10b and 10c, yields the flow vector results of fig. 10e and 10f, respectively. Substituting these flow vectors in (39), and using the global resistance matrices of the members (McGuire and Gallagher, 1979), yields the final result, shown in fig. 10g.

Eq. (39) can also be applied to a continuous graph representation of a structure, i.e. a graph that represents every infinitesimal segment in the structure as if it was a member of its own. This representation is useful when a simple structure subjected to distributed loads is to be analyzed.

Using the right side of (39) will have the following shape:

$$\begin{aligned} \left(\mathbf{F}_R^\Delta\right)^t \cdot \mathbf{R}_R^R \cdot \mathbf{F}_R^F &= \int_{\text{structural segments}} \begin{bmatrix} \mathbf{L} \mathbf{f}^\Delta \\ \mathbf{A} \mathbf{f}^\Delta \end{bmatrix}^t \cdot \begin{bmatrix} \mathbf{T}^t & \circ \\ \circ & \mathbf{T}^t \end{bmatrix}^t \cdot \begin{bmatrix} \mathbf{T}^t & \circ \\ \circ & \mathbf{T}^t \end{bmatrix} \cdot \begin{bmatrix} \mathbf{L}\mathbf{L} \mathbf{R} & \mathbf{A}\mathbf{L} \mathbf{R} \\ \mathbf{L}\mathbf{A} \mathbf{R} & \mathbf{A}\mathbf{A} \mathbf{R} \end{bmatrix} \cdot \begin{bmatrix} \mathbf{T} & \circ \\ \circ & \mathbf{T} \end{bmatrix} \cdot \begin{bmatrix} \mathbf{T}^t & \circ \\ \circ & \mathbf{T}^t \end{bmatrix} \cdot \begin{bmatrix} \mathbf{L} \mathbf{f}^F \\ \mathbf{A} \mathbf{f}^F \end{bmatrix} = \\ &= \int_{\text{structural segments}} \begin{bmatrix} \mathbf{L} \mathbf{f}^\Delta \\ \mathbf{A} \mathbf{f}^\Delta \end{bmatrix}^t \cdot \begin{bmatrix} \mathbf{L}\mathbf{L} \mathbf{R} & \mathbf{A}\mathbf{L} \mathbf{R} \\ \mathbf{L}\mathbf{A} \mathbf{R} & \mathbf{A}\mathbf{A} \mathbf{R} \end{bmatrix} \cdot \begin{bmatrix} \mathbf{L} \mathbf{f}^F \\ \mathbf{A} \mathbf{f}^F \end{bmatrix} \end{aligned} \quad (42)$$

Since each segment has infinitesimal length, dL , high order magnitudes can be eliminated from the internal resistance matrices, and the integration in (42) will then yield the infinitesimal form of (39), as follows:

$$\Pi_{p1}^\Delta = \int_{\text{structural segments}} \left(\frac{\mathbf{L} \mathbf{f}_x^\Delta \cdot \mathbf{L} \mathbf{f}_x^F}{EA} + \frac{\mathbf{A} \mathbf{f}_x^\Delta \cdot \mathbf{A} \mathbf{f}_x^F}{GJ} + \frac{\mathbf{A} \mathbf{f}_y^\Delta \cdot \mathbf{A} \mathbf{f}_y^F}{EI_y} + \frac{\mathbf{A} \mathbf{f}_z^\Delta \cdot \mathbf{A} \mathbf{f}_z^F}{EI_z} \right) \cdot dL \quad (43)$$

which is exactly the formulation known in the literature for the continuous unit-force method (Hibbeler, 1985).

3.3. Deriving the conjugate structure theorems from the mathematical knowledge embedded in graph representations.

Once a structure is represented by a graph representation, all the knowledge embedded in the representation and its relations to other representations become available and can be employed for dealing with the structure. As it was demonstrated in the previous section, this opens up new avenues of research and practical applications in structural research, since the knowledge related to both design and analysis can be imported from other engineering fields.

Current section provides a brief review on an advanced research direction opened through this ability. The idea behind this research is the transformation of a beam or a frame into its dual engineering system through the duality relation between Graph representations.

It is interesting to notice that the same principle has already been applied to establish a duality relation between determinate trusses and mechanisms (Shai, 2001a), which yielded several advancements in solution of diverse engineering problems (Shai, 2002). This relation was established on the basis of the relation between two graph representations - Flow (FGR) and Potential (PGR) Graph Representations. Fig 11 shows an example of a truss and its dual mechanism, together with their corresponding graph representations.

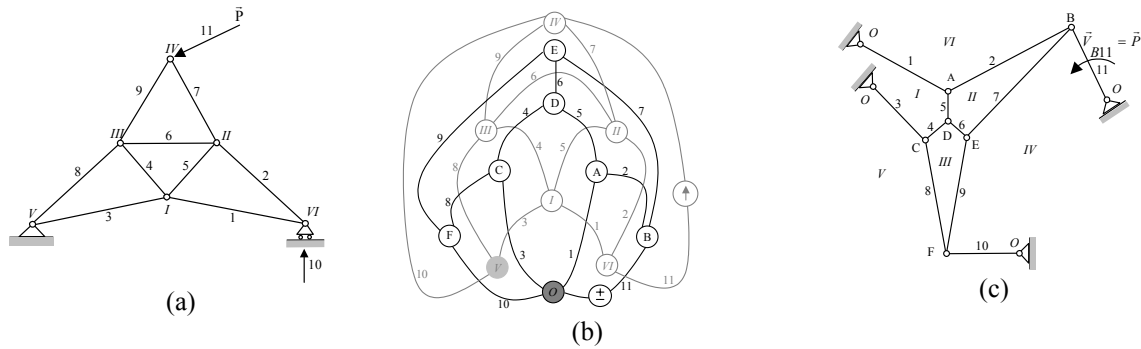


Figure 11. (a) a truss, (b) corresponding graph representation and its dual graph representation and (c) the dual mechanism.

This relation constitutes a powerful tool for translating knowledge between the two engineering fields, thus providing an engineer with an alternative way for dealing with the tasks he faces. It was shown in (Shai2003) that the duality relation can be employed for developing new methods for analysis and design mechanisms and trusses.

Potential Graph Representation and the Flow Graph Representation that were used to establish this relation are known to be components of the Resistance Graph Representation (Shai, 2001b) that has been used here to represent beams and frames. Consequently the duality relations of these representations can be employed for beams and frames as well, as is shown in the following paragraphs.

Consider the fixed supported beam of fig. 12. The displacements in each point along the beam can be represented by a linear and angular potential graphs, ${}^L\mathbf{G}_y^\Delta$ and ${}^A\mathbf{G}_z^\Delta$, whose elements correspond to the infinitesimal segments of the beam, as shown in black in fig. 12b. Although the beam is composed of infinitely large number of segments and so is its PGR, only 4 segments are shown in the figure for clarity.

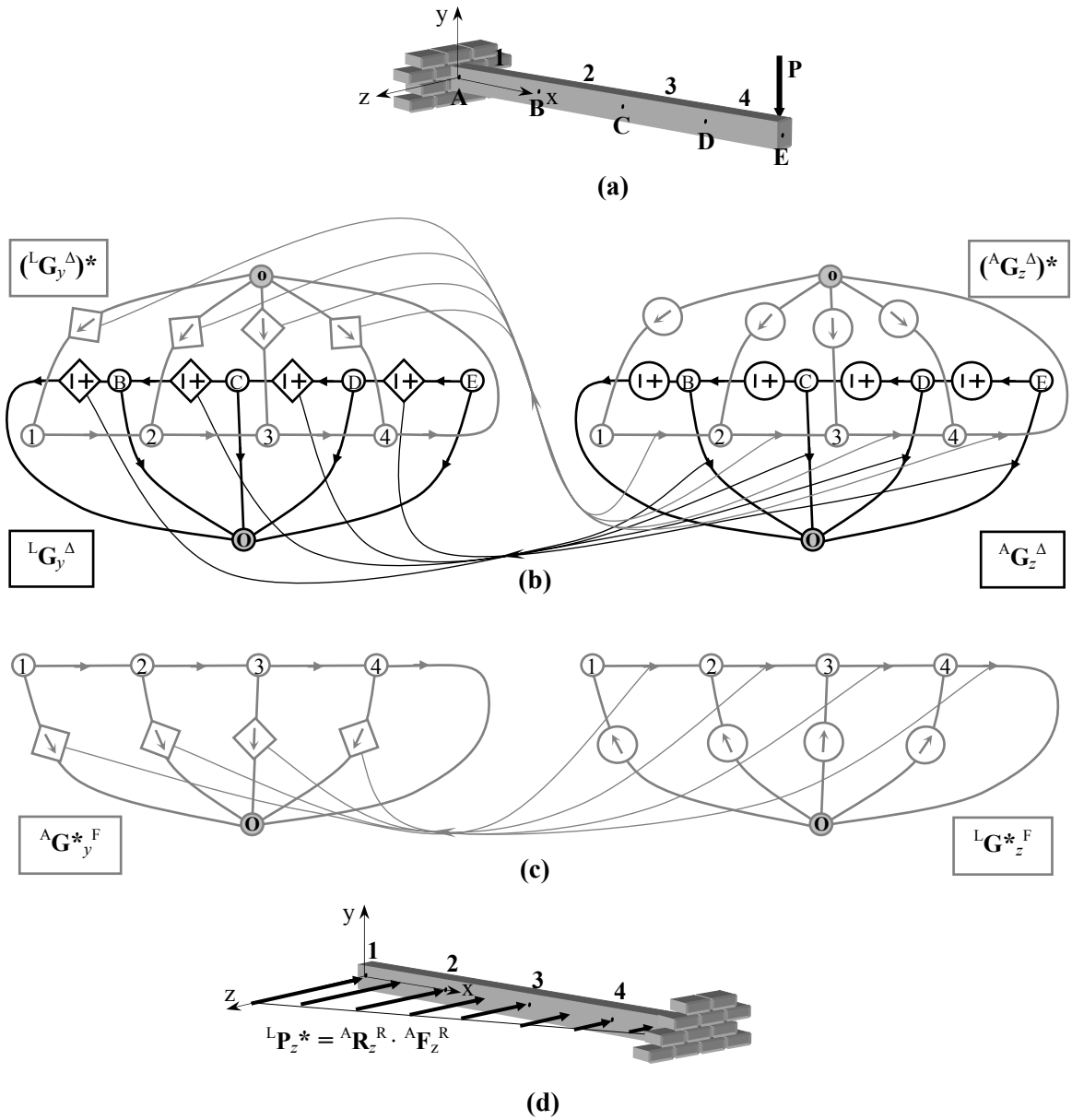


Figure 12. The dual FGR as an FGR of a dual beam

(a) The original beam. (b) The PGR of the original beam (black) and its dual FGR (gray) superimposed. (c) The dual FGR as the flow graph of a dual beam. (d) The dual beam and its external load.

For the potential graph representing the beam one can build a dual graph representation, which was proved to be a Flow Graph Representation, as is shown in Fig 12. One can notice that the obtained flow graph possesses topology typical to the topology of a flow graph representing some beam which is actually the dual engineering system or in other words - the dual beam,.

The dual beam differs from the original one in two aspects: First, the dual beam is clamped at the end which was originally free, while its other end that was originally clamped is free. Second, the externally applied load on the dual beam, shown in fig. 12d, is a distributed load obtained during the construction process, in contrast to the original beam where the external force was applied at a single point

It is interesting to notice that the dual beam is actually the same beam as the one pointed out by Otto C. Mohr in 1860, through his well-known conjugate beam theorem (Hibbeler, 1985). The fact that the dual beam resulted from a determinate procedure over graph representations, indicates a possibility to expand the theorem to more complicated systems, such as frames and to reveal its additional aspects.

3.4. The relation between mechanical structures and integrated systems

As was explained in the introduction, the current paper is aimed on developing graph representations upon which to obtain a system view on structural analysis and not dedicated solely for developing another analysis method based on graph theory. To meet this goal, a graph representation that enables attaining a system perspective on structural analysis has been developed. As was mentioned in the introduction, the skeletal graph representation is similar to the graph representation of integrated system, a relation which opens many avenues of research.

Skeletal structures are widely employed in advanced contemporary technologies such as MEMS, thus applying this representation gives rise to a method of treating this type of engineering systems in a unified way without considering to which engineering domain specific system elements belong.

In order to draw a comparison between the representations of the integrated and the beam systems, Fig. 13 provides examples of these systems and their corresponding graph representations. One can see that the system presented in Fig 13a comprises elements from statics, dynamics and electrical circuits interrelated by means of the control devices. In the corresponding resistance graph representation (Fig. 13b) these control devices are expressed through dependent source edges. As was explained in details throughout the paper and as can be seen from Fig 13d, same dependent source edges are used in the representation of the beam system.

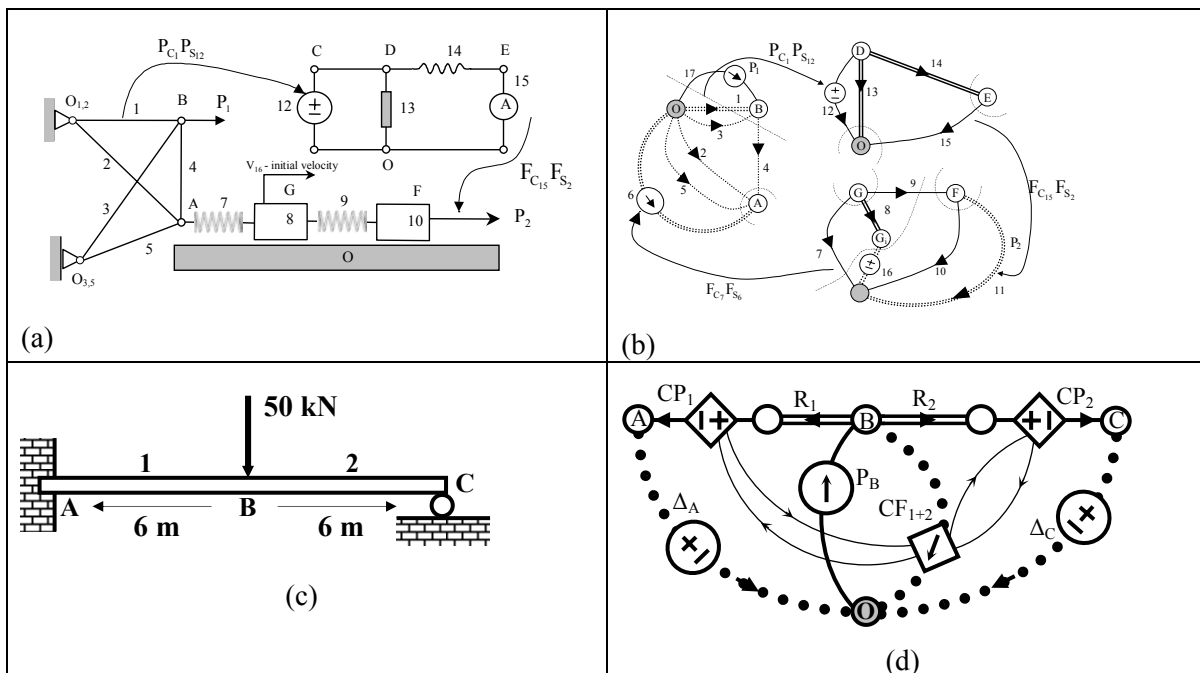


Figure 13. Example integrated and beam systems and their corresponding graph representations.

4. Conclusions and Further Research

The paper has introduced a graph representation to attain a system education perspective on structures and the knowledge embedded in it was adopted and applied to perform the analysis. Due to the generality of the graph representation, all the knowledge embedded in the representation and its relations to other representations become available and can be employed for dealing with the structures. Hence, this representation gives another insight in structural engineering education, since the knowledge related to both design and analysis can be taught through the mathematical basis of the graph representations. The approach of teaching structural mechanics from a multidisciplinary system perspective has already been tested with high school students, and outstanding results were achieved (Shai, 2001b).

Additional aspect of the approach is enabling the students to witness how the mathematical laws of graph theory are reflected in the laws underlying the physical behavior of structures. Two preliminary results of such derivations have been reported: The well-known Tellegen's theorem from electricity was applied to the Resistance Graph Representation of a structure, and it was shown that the result coincides with a well-known mechanical energy method – the unit-force method. In the same section, it was shown that through the duality relation between Graph Representations, the transformation of a beam into its dual engineering system results with a dual beam that is actually the same as the one pointed out by Otto C. Mohr in 1860, through his well-known conjugate beam theorem (Hibbeler, 1985). The fact that the dual beam resulted after applying a determinate procedure to graph representations gives the students an insight upon the derivation of known theorems and methods from more general mathematical laws.

The research work shown in the paper is expected to be applicable in many ways, including transferring engineering knowledge from other engineering fields into structural mechanics and vice versa. This indicates that the students will gain their understanding not only in structural

mechanics , but also in other engineering domains that are represented by the same graph representation.

It should be emphasized that the work reported in this paper is a part of a more general research approach called Multidisciplinary Combinatorial Approach (MCA), summarizing the results of previous publications on applying graph theory to engineering into a general graph representation framework. The same type of graph as the one employed in this paper, has been employed also in MEMS (Shai et. al. 2002), integrated systems (Shai and Rubin, 2003), robotics (Shai, 2002b), and other advanced topics of modern engineering.

5. References

- Andrews G.C., 1971. The Vector-Network Model - a Topological Approach to Mechanics. Ph.D. thesis, University of Waterloo.
- Balabanian, N.; Bickart, T. A., 1969. Electrical Network Theory. New York, John Wiley & Sons.
- Bjørke Ø., 1995. Manufacturing Systems Theory – A Geometric Approach to Connection, Tapir Publishers, Norway.
- Carter G.K. and Kron G., 1944. Network Analyzer Solution of the Equivalent Circuits for Elastic Structures, *Journal of the Franklin Institute*, 238(6), 442-452.
- Fenves S.J. and Branin F.H.Jr., 1963. Network-Topological Formulation of Structural Analysis, *Journal of the Structural Division*, ASCE 89 (ST4), 483-514.
- Fenves S.J., Logcher R.D., Mauch S.P. and Reinschmidt K.F., 1964. *STRESS – A User's Manual*, MIT Press, Cambridge, MA.
- Fleming J.F., 1989. *Computer Analysis of Structural System*, McGraw-Hill, New York.
- Fuchs M.B., 1992. The Explicit Expression of Internal Forces in Prismatic Member Structures, *Journal of Mechanical Structures and Machines*, 20(2), 169-194.
- Goldstein H., 1950. *Classical Mechanics*, Addison-Wesley Publishing Company, Inc., Manila.
- Hibbeler R.C., 1985. *Structural Analysis*, Macmillan Publishing Company, New York.
- Kaveh A, 1995. *Structural Mechanics: Graph and Matrix Methods*, 2nd Ed., Research Studies Press Ltd, Somerset.
- Kron G., 1963. Diakoptics – A Piecewise Solution of Large-Scale Systems, Macdonald, London.
- Langefors B., 1961. Algebraic Topology for Elastic Networks, *SAAB Technical Notes*, TN49.
- McGuire W. and Gallagher R.H., 1979. *Matrix Structural Analysis*, John Wiley & Sons Inc., New York.
- Roth J.P., 1955. An Application of Algebraic Topology to Numerical Analysis: On the Existence of a Solution to the Network Problem, *Proceedings of the National Academy of Science*, 41(7), 518-521.
- Shai O., 2001a. The Duality Relation between Mechanisms and Trusses, *Journal of Mechanism and Machine Theory*, 36(3), 343-369.
- Shai O., 2001b. Combinatorial Representations in Structural Analysis, *Journal Computing in Civil Engineering*, 15(3), 193-207.
- Shai O., 2001c, "Deriving Structural Theorems and Methods Using Tellegen's Theorem and Combinatorial Representations", *International Journal of Solids and Structures*, Vol. 38, pp. 8037-8052,
- Shai O., 2002, "Duality between Statical and Kinematical Engineering Systems", *The Sixth International Conference on Computational Structures Technology*, Prague, Czech Republic, 4-6 September.

- Shai O., 2003, "Transforming Engineering Problems through Graph Representations", *Advanced Engineering Informatics*, Vol. 17, No. 2, pp. 77 - 93.
- Shai O., Eliahou-Niv S., Rubin D., Slavutin M. and Andrusier A., 2002, "Multidimensional Graph Representations for MEMS and their Applications", *ISRAMEMS – the 1st National Conference of the Israeli MOEMS Society*, Haifa, Israel.
- Shai O. and Preiss K., "Isomorphic Representations and Well-Formedness of Engineering Systems", *Engineering with Computers*, Vol. 15, pp. 303-314, 1999.
- Southwell R.V., 1940. *Relaxation Methods in Engineering Science*, Oxford University Press, London.
- Spillers W. R., 1963. Network Analogy for Linear Structures, *Journal of the Engineering Mechanics Division, Proceedings of The ASCE*, 89 (EM4), 21-29.
- Swamy M.N.S. and Thulasiraman K., 1981. *Graphs, Networks, and Algorithms*, John Wiley & sons Inc., New York.
- Ta'aseh N. and Shai O., 2002, "Derivation of Methods and Knowledge in Structures by Combinatorial Representations", *The Sixth International Conference on Computational Structures Technology*, Prague, Czech Republic.
- Tellegen, B.D.H., 1952. A general network theorem with applications. *Philips Res. Rep.* 7, 259-269.
- Wang K. and Bjørke Ø., 1991. Mechanical Networks Model for the Plane Frame System, *Journal of Computers In Industry*, 16, 113-128.